Probing the parameter constraints on astrophysical environments of intermediate and extreme mass ratio inspiral binaries with LISA

Marco Immanuel B. Rivera* and Reinabelle C. Reyes

National Institute of Physics, University of the Philippines Diliman, Quezon City 1101, Philippines
*Corresponding author: mrivera@nip.upd.edu.ph

Abstract

The future space-borne Laser Interferometer Space Antenna (LISA) would allow detection of intermediate (IMRI) and extreme mass ratio inspirals (EMRI) via their gravitational wave (GW) emission. However, these binaries may live in nontrivial astrophysical environments, affecting their GW emission and thereby complicating detection and parameter estimation. By using Fisher matrix analysis, we calculate the uncertainties in the environmental density of inspirals with different mass ratios. We study several environmental effects affecting GW emission – gravitational pull, collisionless accretion, and gravitational drag – and find a log-log relationship between the uncertainties and the primary mass of the binary. By using overlap analysis, we also get the signal-to-noise ratios (SNR) of the difference between a vacuum and an environmentally-modified waveform. We find that the dephasing brought about by environmental effects may be detectable within LISA's 4-year mission lifetime, especially for EMRIs.

Keywords: gravitational waves, LISA, Fisher matrix analysis, overlap analysis

1 Introduction

The planned Laser Interferometer Space Antenna (LISA) will be able to detect extreme mass ratio inspiral (EMRI) binaries [1]. These kinds of binaries spend a lot of time in their inspiral phase, which allows us to accurately describe the spacetime [1] and astrophysical environment [2] around the massive black hole. Previous work has shown that including environmental effects in the waveform – namely gravitational pull, collisionless accretion, and gravitational drag – would allow LISA to constrain the surrounding (constant) medium's density by up to 10^{-7} kg/m^3, 10^{-13} kg/m^3, and 10^{-22} kg/m^3, respectively, for EMRIs with mass ratio $q \equiv m_1/m_2 = 10^4$ [3]. These values were obtained from the covariance matrix, which is the inverse of the Fisher information matrix in the limit of high signal-to-noise ratio (SNR). This Fisher information analysis has been extensively used in gravitational-wave astronomy to determine if planned detectors can accurately extract information from their specified targets [4].

In this paper, we extend the analysis in [3] to binaries of varying mass ratios to see how the uncertainties in measuring the environmental density depend on the primary mass of the binary. In effect, we are studying the manifold space of a waveform with dephasing from environmental effects. Since this space consists of many dimensions, we set some parameters constant such as the secondary mass ($m_2 = 10\ M_\odot$), primary spin ($\chi_1 = 0.8$), secondary spin ($\chi_2 = 0.5$), and the luminosity distance of the binary ($d_L = 1$ Gpc). Here, $\chi_i = (c/G)S/m_i^2$ is the dimensionless spin angular momentum of the ith compact object [5]. In particular, we look for trends in the uncertainty of the surrounding medium's density over a range of primary masses for several environmental effects. Furthermore, using overlap analysis, we determine how different the vacuum and dephased waveforms would be for LISA by estimating the SNR of the waveform difference.

2 Methodology

2.1 Setup

We simulated several inspiralling quasi-circular compact binaries living in an astrophysical environment of constant density ρ_0. In general, we can assume that the orbit evolves adiabatically so that any changes in its motion due to environmental effects can be perturbatively added to the vacuum case, and that the accretion timescale is much longer than the observation time so that both the black hole mass and environmental density do not change significantly as the binary enters the LISA bandwidth [2]. This allows us to construct frequency-domain vacuum waveforms within the stationary phase approximation (SPA), given by $\tilde{h}(f) = \mathcal{A}(f)e^{i\Psi(f)}$. Since we are working exclusively in the LISA frequency spectrum, we restrict our attention to black hole-black hole (BH-BH) binaries: in particular, intermediate (with

$q \in [10^1, 10^3]$) and extreme (with $q \in [10^4, 10^5]$) mass ratio inspirals. We created a phenomenological inspiral-merger-ringdown (IMRPhenomB) waveform [6] for the GW phase Ψ of a BH-BH binary with nonprecessing spins. We also adapted Berti et. al's "restricted post-Newtonian (PN) approximation" [7] for the amplitude $\mathcal{A}$.

To construct the environmentally-modified waveform, we used the parametrized post-Einsteinian (ppE) formulation [8] by multiplying the dephasing factor $\exp(i\psi_{\rm env}) = \exp(i\psi_{\rm GR}\delta_{\psi_{\rm env}})$ to the vacuum IMRPhenomB waveform. Here $\psi_{\rm GR} = 3/128(\mathcal{M}\pi f)^{-5/3}$ is the leading term in the PN expansion of the phase, $\mathcal{M} = M\eta^{3/5}$ is the chirp mass of the binary, $M \equiv m_1 + m_2$ is the total mass of the binary, $\eta \equiv (m_1 m_2)/M^2$ is the symmetric mass ratio, and f is the GW frequency. The dephasing factors depend on the type of environmental effect considered. They were calculated in a perturbative manner by considering the linear term in the density and adding it to the Newtonian potential [2, 3]. These effects were considered independently of one another even though they might occur together in astrophysical environments. We use the following $\delta_{\psi_{\rm env}}$ for a surrounding medium of constant density ρ_0: $\delta_{\psi_{\rm pull}}(f) = f^{-2}\rho_0$, $\delta_{\psi_{\rm drag}}(f) = -\eta^{-3}(1-3\eta)\pi^{-11/3}M^{-5/3}f^{-11/3}\rho_0$, and $\delta_{\psi_{\rm collisionless}}(f) = -\eta^{-1}\pi^{-3}M^{-1}f^{-3}\rho_0$ [3]. Here, "pull" stands for the gravitational pull of the surrounding medium inside the orbital radius (centered at the binary's center of mass), "drag" stands for the gravitational drag (without dephasing from dynamical friction) from the surrounding medium, and "collisionless" stands for the collisionless accretion of the surrounding medium onto the central BH.

2.2 Fisher matrix calculation

We calculate the Fisher matrix elements Γ_{ij} as the overlap integral $\mathcal{O}\left(\frac{\partial\tilde{h}}{\partial\theta_i}\middle|\frac{\partial\tilde{h}}{\partial\theta_j}\right)$ [9] between the derivatives of the modified strain with respect to the relevant waveform parameters θ_i, hereby listed with their fiducial values: $\{\ln\mathcal{M}/M_\odot, \ln\eta, \tau_c = 0, \phi_c = -\pi/4, \chi_{\rm eff}, \rho_0 = 0\}$. Here, τ_c represents the time at coalescence, ϕ_c the phase at coalescence, and $\chi_{\rm eff} = (\chi_1 m_1 + \chi_2 m_2)/M$ the effective spin parameter. Explicitly,

$$\Gamma_{ij} = \mathcal{O}\left(\frac{\partial\tilde{h}}{\partial\theta_i}\middle|\frac{\partial\tilde{h}}{\partial\theta_j}\right) = 4\,\mathrm{Re}\int_{f_{\rm min}}^{f_{\rm max}} \frac{df}{S_n(f)}\frac{\partial\tilde{h}}{\partial\theta_i}\left(\frac{\partial\tilde{h}}{\partial\theta_j}\right)^*, \tag{1}$$

where Re denotes taking the real part, * denotes conjugation, and $S_n(f)$ is the power spectral density (PSD) of LISA [10]. The limits of integration are chosen such that the lower bound may be dependent on the time of observation $T_{\rm obs}$ [7], while the upper bound may be dependent on f_1: the inspiral-merger transition frequency from Ajith et. al's semi-analytical IMRPhenomB model [6]. They are given by $f_{\rm min} = \max\left[10^{-5},\ 4.149\times10^{-5}\left(\frac{\mathcal{M}}{10^6 M_\odot}\right)^{-5/8}\left(\frac{T_{\rm obs}}{1\rm yr}\right)^{-3/8}\right]$ Hz and $f_{\rm max} = \min[1, f_1]$ Hz. For these calculations, we set $T_{\rm obs} = 4$ years. From Γ_{ij}, we can calculate the standard deviation σ^i by inverting the Fisher matrix to get the covariance matrix $\Sigma^{ij} = (\Gamma^{-1})^{ij}$ and getting the square root of the diagonals: $\sigma^i = \sqrt{\Sigma^{ii}}$ [4, 9].

2.3 Signal-to-noise ratio (SNR) of the waveform difference

To get the SNR of the waveform difference, we use the expression for the optimal SNR [9, 11]. We then make the SNR a function of $T_{\rm obs}$ to see how it accumulates over time. For two waveforms $\tilde{h}_1$ (the signal) and $\tilde{h}_2 = \tilde{h}_1\exp(i\psi_{\rm env})$ (the dephased waveform template where we set $\rho_0 = 10^3$ kg/m^3), the SNR of the waveform difference is given by

$$\left(\frac{S}{N}\right)^2 = \mathcal{O}(\tilde{h}_1 - \tilde{h}_2|\tilde{h}_1 - \tilde{h}_2) = 4\,\mathrm{Re}\int\frac{|\tilde{h}_1(f) - \tilde{h}_2(f)|^2}{S_n(f)}df = 8\,\mathrm{Re}\int_{f_{\rm min}}^{f_{\rm max}}\frac{|\tilde{h}_1|^2}{S_n(f)}[1-\cos(\psi_{\rm env})]\,df. \tag{2}$$

3 Results and Discussion

Table 1 shows the source parameters $\mathcal{M}$, η, $\chi_{\rm eff}$, $f_{\rm min}$ and $f_{\rm max}$, as well as the number of completed orbital cycles for five simulated binaries with primary masses $m_1 \in \{10^2, 10^3, 10^4, 10^5, 10^6\}$ $M_\odot$. These values enter the waveform construction and overlap calculations. We note that the calculations fail for $m_1 \geq 10^7$ $M_\odot$ since the detectable waveform is already past the inspiral phase ($f_{\rm min} > f_{\rm max}$). We also note that Ajith et. al's IMRPhenomB model is not calibrated for higher mass ratios.

From the calculated covariance matrices, we obtained the uncertainties of the surrounding density σ_{ρ_0} marginalized over the other waveform parameters. We plot the values of $\log\sigma_{\rho_0}$ against $\log m_1$

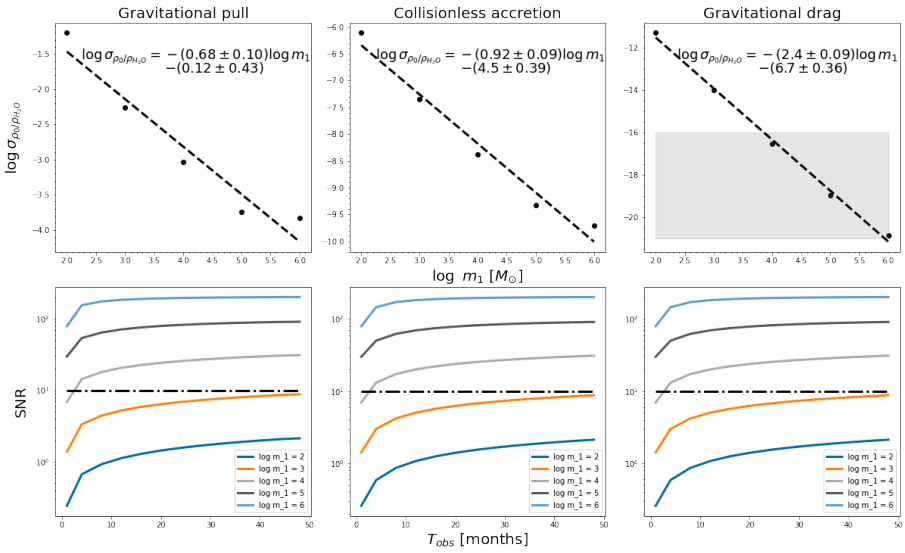

Figure 1: (Top row) 1-σ uncertainties for the density of the surrounding medium (normalized to water density) as a function of the primary mass of the simulated binaries. The density range typical of accretion disks span $\rho_0/\rho_{\mathrm{H_2O}} \in [10^{-16}, 10^{-1}]$, while the density range typical of dark matter span $\rho_0/\rho_{\mathrm{H_2O}} \in [10^{-25}, 10^{-16}]$ (shaded gray region). Also shown are the best-fit log-log relationships (dashed lines). (Bottom row) Signal-to-noise ratio of the difference between the vacuum IMRPhenomB waveform and environmentally-modified waveform as a function of observation time for different primary masses. The modified waveforms used are for binaries living in $\rho_0 = 10^3$ kg/m^3 environments. The dot-dash line indicates the conservative SNR estimate for signal detection.

for the three environmental effects in the top row of Figure 1. We find that the uncertainties in the density of the surrounding medium follow an inverse log-log relationship with the primary mass, with the following best-fit exponents for gravitational pull, collisionless accretion, and gravitational drag, respectively: -0.68 ± 0.10, -0.92 ± 0.09, and -2.4 ± 0.09. These results partially define the structure of the complete 6-dimensional covariance ellipsoid spanning the waveform parameter space. We note that as expected for all environmental effects, we were able to recover Cardoso and Maselli's results for $m_1 = 10^4\ M_\odot$ and $m_1 = 10^5\ M_\odot$ [3].

We see that for the same primary masses, different environmental effects lead to different magnitudes of σ_{ρ_0}. Gravitational drag leads to the tightest constraints, probing densities typical of dark matter for $m_1 \geq 10^4\ M_\odot$ (in the shaded gray region of Figure 1). At this point we emphasize that in our calculations, the different environmental effects were considered independent of one another. This may be different from the realistic astrophysical scenario in which all three (as well as other effects) come into play.

The SNR calculations indicate that for the higher primary masses $10^4 - 10^6\ M_\odot$, the difference between a vacuum and dephased waveform would be (almost instantly) visible to LISA, as seen in the bottom row of Figure 1. This means that using a vacuum waveform template to match a signal with environmental dephasing may hamper detection, in agreement with the findings of Kocsis et. al [11] for other waveform

Table 1: Chirp mass $\mathcal{M}$, symmetric mass ratio η, effective spin χ_{eff}, minimum and maximum frequencies for the overlap integrals, and the number of orbital cycles for five simulated binaries. For each primary mass, we set other source parameters constant: $m_2/M_\odot = 10$, $\chi_1 = 0.8$, and $\chi_2 = 0.5$. We adapt the notation $x(y) = x \times 10^y$.

$\log m_1/M_\odot$	$\mathcal{M}/M_\odot$	η	χ_{eff}	f_{min} [Hz]	f_{max} [Hz]	no. of cycles
2.0	2.46(1)	8.26(−2)	7.72(−1)	1.87(−2)	1.00(0)	3.75(6)
3.0	6.30(1)	9.80(−3)	7.97(−1)	1.04(−2)	1.00(0)	2.09(6)
4.0	1.58(2)	9.98(−4)	8.00(−1)	5.85(−3)	1.00(0)	1.17(6)
5.0	3.98(2)	9.99(−5)	8.00(−1)	3.29(−3)	1.13(−1)	6.58(5)
6.0	9.99(2)	1.00(−5)	8.00(−1)	1.85(−3)	1.13(−2)	3.53(5)

and dephasing models.

For the simulated IMRI binaries, on the other hand, dephased and vacuum waveforms cannot be distinguished from each other, even after four years of observation. This might mean we cannot use LISA to recover the nature of our binaries' astrophysical environments. For all environmental effects affecting the binary with $m_1 = 10^3\ M_\odot$, we find that the SNR of the waveform difference reaches the threshold of detection towards the end of the 4-year observation period. The difference would be detectable for sources that are closer than our reference luminosity distance of 1 Gpc, since the SNR scales as $1/d_L$.

4 Conclusions and recommendations

In this paper, we have shown how LISA can distinguish the environment around IMRI/EMRI binaries using Fisher matrix analysis and overlap analysis of vacuum and environmentally-dephased waveforms. These calculations can be used as a starting point in mapping the confidence intervals around the waveforms' true parameters, towards getting better estimates of the binary's environmental and source parameters.

We can improve the analysis by checking for trends on the other source parameters to complete the confidence intervals. It would also be better to use more accurate frequency domain waveforms for EMRIs with higher q [12]. We can also use the Fisher matrix of the PN (and ppE) parameters to obtain better constraints and determine degeneracies among waveform parameters [13]. Other dephasing models for environmental effects such as those considered in [11] may also be studied. Finally, the assumption on the structure of the surrounding medium can be relaxed and more generic density profiles such as dark matter power-law distributions (which make the surrounding medium's effects depend on its distance from the central BH) [3] may be further studied.

Acknowledgments

The authors would like to acknowledge the helpful discussions and inputs from the following: Ian Vega, Adrian Villanueva, Bence Kocsis, Nico Yunes, Abraham Loeb, and anonymous SPP reviewer. The authors also acknowledge the use of code generously provided by Vitor Cardoso and Andrea Maselli.

References

[1] P. Amaro-Seoane et al., Laser Interferometer Space Antenna (2017), arXiv:1702.00786.

[2] E. Barausse, V. Cardoso, and P. Pani, Can environmental effects spoil precision gravitational-wave astrophysics?, *Phys. Rev. D* **89**, 104059 (2014).

[3] V. Cardoso and A. Maselli, Constraints on the astrophysical environment of binaries with gravitational-wave observations, *Astron. Astrophys.* **644**, A147 (2020).

[4] M. Vallisneri, Use and abuse of the Fisher information matrix in the assessment of gravitational-wave parameter-estimation prospects, *Phys. Rev. D.* **77**, 042001 (2008).

[5] LIGO Scientific and VIRGO Collaborations et al., The basic physics of the binary black hole merger GW150914, *Ann. Phys.* **529**, 1600209 (2017).

[6] P. Ajith et al., Inspiral-merger-ringdown waveforms for black-hole binaries with nonprecessing spins, *Phys. Rev. Lett.* **106**, 241101 (2011).

[7] E. Berti, A. Buonanno, and C. M. Will, Estimating spinning binary parameters and testing alternative theories of gravity with LISA, *Phys. Rev. D.* **71**, 084025 (2005).

[8] N. Yunes and F. Pretorius, Fundamental theoretical bias in gravitational wave astrophysics and the parametrized post-einsteinian framework, *Phys. Rev. D.* **80**, 122003 (2009).

[9] M. Maggiore, *Gravitational waves: Volume 1: Theory and experiments* (Oxford University Press, New York, 2008).

[10] T. Robson, N. J. Cornish, and C. Liug, The construction and use of LISA sensitivity curves, *Class. Quantum Grav.* **36**, 105011 (2019).

[11] B. Kocsis, N. Yunes, and A. Loeb, Observable signatures of extreme mass-ratio inspiral black hole binaries embedded in thin accretion disks, *Phys. Rev. D.* **84**, 024032 (2011).

[12] S. Isoyama, R. Sturani, and H. Nakano, Post-Newtonian templates for gravitational waves from compact binary inspirals, in *Handbook of Gravitational Wave Astronomy*, edited by C. Bambi, S. Katsanevas, and K. D. Kokkotas (Springer, Singapore, 2020), 1–49, arXiv:2012.01350.

[13] F. Ohme, A. B. Nielsen, D. Keppel, and A. Lundgren, Statistical and systematic errors for gravitational-wave inspiral signals: A principal component analysis, *Phys. Rev. D* **88**, 042002 (2013).